SCIENCE CHINA
Technological Sciences

June 2011 Vol.54 No.6: 1382–1388
doi: 10.1007/s11431-011-4405-1

In situ investigation of SiC powder's microwave sintering by SR-CT technique

LI YongCun[1], XU Feng[1*], HU XiaoFang[1], QU HongYan[1], MIAO Hong[1], ZHANG Zhong[2] & XIAO TiQiao[3]

[1] *Chinese Academy Sciences Key Laboratory of Mechanical Behavior and Design of Materials, University of Science and Technology of China, Hefei 230026, China;*
[2] *National Center for Nanoscience and Technology of China, Beijing 100190, China;*
[3] *Shanghai Synchrotron Radiation Facility, Shanghai 201204, China*

Received January 27, 2011; accepted March 2, 2011; published online April 20, 2011

Microwave sintering is being developed as a novel technique for the preparation of dense structural ceramics, but the mature theory has not been established due to the technical difficulties. The synchrotron radiation X-ray computed tomography (SR-CT) technique was introduced for the first time into the study of microwave sintering to in-situ observe the microstructure evolution of silicon carbide (SiC) material in this paper. By applying the SR-CT technique, the reconstructed 2D and 3D images of the specimen were obtained and the double logarithm curve of mean neck size and time (Ln(x)-Ln(t)) were obtained from these reconstructed images. Various sintering phenomena including sintering neck growth during microwave treatment were observed from the reconstructed images. Furthermore, the differences in microstructure evolution and sintering kinetics between microwave and conventional sintering were analyzed based on the reconstructed images and the Ln(x)-Ln(t) curve. 1) The sharp surface of grains near the contact region distinctly grew blunt and the sintering neck growth between these grains were obviously observed at the early stage. Besides, the larger particles grew faster than smaller ones. The main reason for these phenomena may be the micro-focusing effect of electric fields. 2) During each of the three sintering stages, the sintering kinetics curve of double logarithm relationship between mean neck size and time shows a good linear relationship, but at the middle stage the slope of the curve increases dramatically, which is quite larger than conventional sintering. The preliminary interpretation for these extraordinary phenomena has been discussed in details.

silicon carbide, synchrotron radiation X-ray computed tomography, microwave sintering

Citation: Li Y C, Xu F, Hu X F, et al. *In situ* investigation of SiC powder's microwave sintering by SR-CT technique. Sci China Tech Sci, 2011, 54: 1382–1388, doi: 10.1007/s11431-011-4405-1

1 Introduction

Microwave sintering develops as a novel technique for the preparation of structural ceramics and achieves the high-temperature sintering depending on the material's dielectric loss in the microwave field. It features densification process enhancement, less sintering time and decreasing grain-size of products compared with conventional sintering, and has been successfully applied to sinter various materials such as Al_2O_3 [1, 2], Si_3N_4 [3] and ZnO [4] for rapid heating and improvement of microstructures of materials. However, as the high-temperature electromagnetism field and microwave radiation restrict the experimental investigation on the microstructure evolution characteristics by traditional techniques, an accepted mature theory of microwave sintering

*Corresponding author (email: xufeng3@ustc.edu.cn)

has not been established. There are some optical and electron microscopy techniques generally applied to investigate the microstructure characteristics of ceramic materials such as high resolution transmission electron microscope (HR-TEM) and scanning electron microscopy (SEM), which can only acquire high resolution images of the microstructure of internal fracture surface and super-thin slice. Not only do these techniques destroy the original microstructure, but fail to observe the characteristics of microstructure evolution process online, for example, porosity decrease, sintering neck and grain growth during the microwave sintering. Therefore, it is tremendously helpful to explore an appropriate experimental method to support the mechanism revelation and process optimization of microwave sintering.

SR-CT technique [5–7] is a latest non-destructive detection technology. By applying this technique, in-situ observation of microstructure evolution of materials under the extreme conditions (e.g., high temperature, high pressure, intense radiation, etc.) becomes possible. Applying the SR-CT technique to the research of microwave sintering can realize the observation of the evolution of microstructures under microwave and high-temperature field in a non- destructive, 3D and real-time way, can provide more accurate experiment data for revealing the kinetics mechanism of microstructure evolution, and can offer direct foundation for establishing the theory of microwave sintering.

For the limitations of experimental skills, especially due to the high-temperature environment and the intense microwave radiation, it is difficult to use the SR-CT technique to observe the microstructure evolution process during microwave sintering. At present, researchers only carry out the SR-CT experiments on conventional sintering. Vagnon et al. did research on stress varying during conventional sintering process of steel powder compacts by SR-CT [8]. Lame et al. [9] applied SR-CT technique to observing the sintering process of Cu powders at 1050°C and steel powders at 1130°C. Neck formation and particle rearrangement were clearly observed in their work [10]. Grain evolution of boron carbide powders was observed and discussed by using SR-CT technique [11].

In this paper, we overcame the difficulties in the application of the SR-CT technique to microwave sintering, and we firstly used the SR-CT method to in-situ investigate the microstructure evolution of silicon carbide powders during microwave sintering. Using filtered back projection reconstruction algorithm and digital image processing method to reconstruct the 2D and 3D images of the internal microstructure of specimen at different sintering times, the sintering phenomena during microwave sintering, including the shape change of grain surface, the sintering neck formation and growth have been clearly observed from the reconstructed images. Compared with the conventional sintering, the neck grew much more rapidly and the sharp surface near the contact regions distinctly turned blunt. The double logarithm curve of mean neck size and time was obtained, from which a rapid sintering neck growth stage was discovered. The preliminary interpretation for these extraordinary phenomena such as the micro-focusing of electric fields has been discussed in detail.

2 Experiment

2.1 Brief introduction of SR-CT technical

SR-CT technique is a non-destructive testing method by which the specimen was passed through by synchrotron radiation X-ray is placed in a rotation and the projection images of the specimen are received by an X-ray charge-coupled device (CCD). One projection image is collected each time when the specimen turns by an angle. After obtaining a set of projection data, reconstruction algorithm is used to obtain the internal microstructure of the sectional images. The 3D image of the microstructure can be obtained from a series of sectional images. Reconstruction algorithms applied in SR-CT technique are mainly the filtered by back projection and iterative algorithms. Taking the limited time into account, we employed the filtered back projection algorithm in this paper.

2.2 Experimental procedure

In our experiment, a packing of chemically pure SiC (99.9%) powders with the average diameter of 125 μm has been investigated. The experiment was carried out on the BL13W1 beam line at Shanghai Synchrotron Radiation Facility (SSRF, China). The energy of the beam ranged from 8 to 72 keV. Considering the X-ray absorption coefficient of SiC, an X-ray with 20 keV selected by silicon single-crystal monochromatic was applied. Schematics of the SR-CT experimental setup is shown in Figure 1.

The synchrotron radiation X-ray passed through the specimen and reached an X-ray CCD detector which recorded the intensity message of X-ray. The CCD including a 4000 pixels×2500 pixels chip with a unit pixel of 7 μm × 7 μm offered a 12-bit dynamic range. A 2.45 GHz microwave generator with the output power from 0 to 3 kW was used as microwave source, the typical microwave heating profile is shown in Figure 2. The MRS102 rotation device with angle resolution of 0.00125° and repeatable positioning accuracy of 0.005° was provided by the Beijing Optical Instrument Factory. The SiC powders were poured into a 2.5 mm-diameter, 30 mm-height quartz capillary and introduced into a specially designed microwave sintering furnace. At different sintering times, the specimen was imaged at different projection angles (in the range of 0°–180°). Typically, 180 shadow images of the specimen were acquired and then processed by the filtered back projection algorithm.

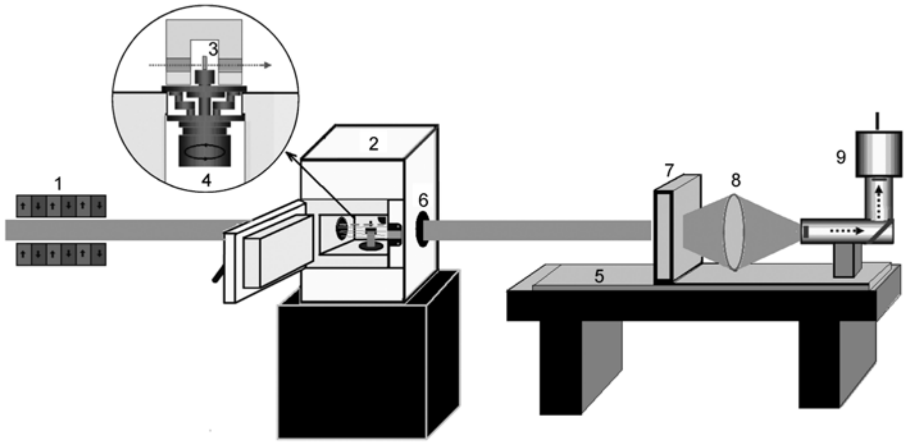

Figure 1 Schematic diagram of SR-CT Projection Imaging Facility. 1, X-ray source; 2, microwave sintering furnace; 3, sample; 4, rotation device; 5, anti-vibration platform; 6, holes; 7, fluorescent target; 8, optical; 9, X-Ray CCD.

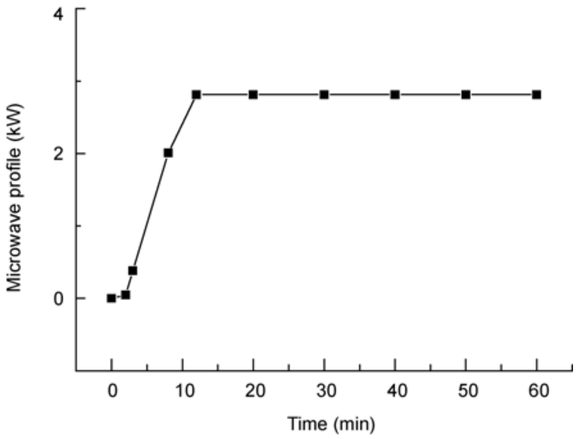

Figure 2 Microwave heating power.

3 Results

By the marks on the specimen and the correlation algorithm, we found the same cross-section images at different sintering times. The reconstructed images of the same cross- section at different times are shown in Figure 3. Grayscale ranges from 0 to 255; the closer to 255, the higher the relative density, which means white represents particles and black represents holes.

Vertical-section and 3D reconstructed images can also be obtained by treating the cross-section images with digital image processing method. By applying 3D reconstruction algorithm, a series of cross-section images were assembled to obtain a 3D image and the section in any position of the specimen, as shown in Figure 4.

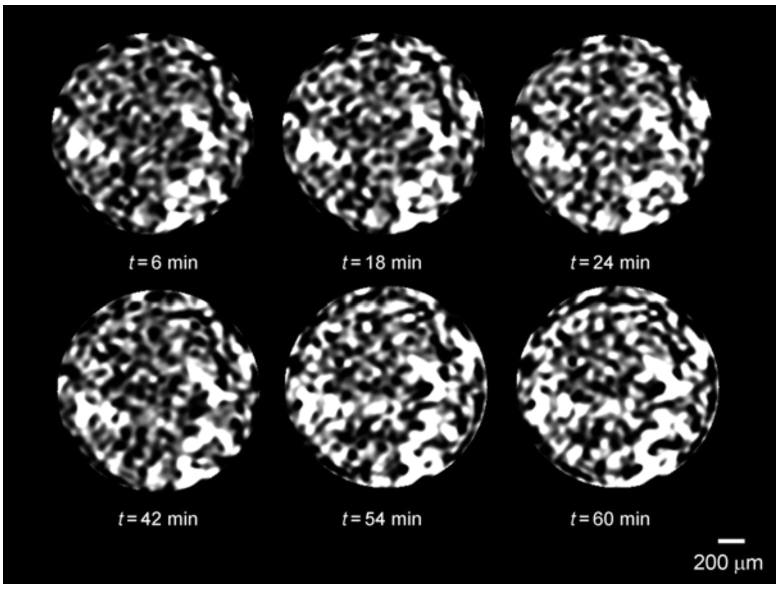

Figure 3 Reconstructed images of the same cross-section of the sample in different sintering periods.

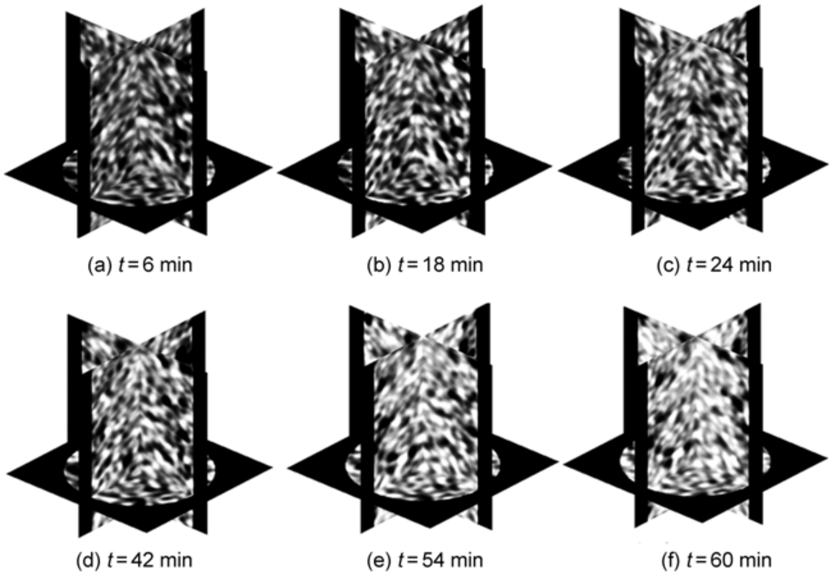

Figure 4 Sectional views in different directions.

Figure 5 shows the 3D reconstructed images of the specimen, from which the 3D morphology evolution of the specimen by increasing the sintering time can be clearly observed.

4 Discussion

As described in section 1, microwave sintering has many attractive features compared with the conventional sintering, and there are many different characteristics between the two sintering techniques, such as the heating mechanism, heat conduction manner, mass diffusion mechanism, etc. In this section, the difference of microstructure evolution process and sintering neck growth between them will be discussed.

4.1 Difference in microstructure evolution

Microstructure is one of the most important factors that affect ceramic's properties like density, rigidity, mechanical

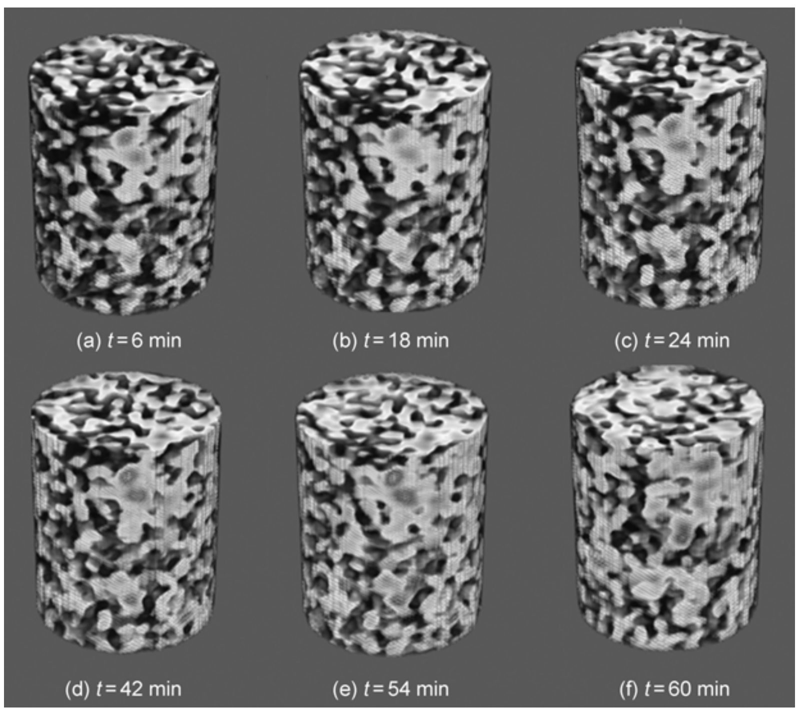

Figure 5 Three-dimensional reconstructed images of the sample at different sintering times.

properties, etc. The ceramic's final microstructure is largely determined by the microstructure evolution process, such as sintering neck formation and growth, grain growth, pore isolation and spheroidization. As reported [12–14] in many studies, the ceramic products processed by microwave sintering have some obvious differences from conventional sintering, such as the grain size and its uniformity, the shape and the amount of pores. So there must be some differences of microstructure evolution behavior between them. Due to the limitations of experimental skills, especially the high temperature environment and the intense microwave radiation, it is difficult to observe the microstructure evolution process by traditional experimental techniques. In our experiment, the SR-CT technique was used to observe this process, and some distinct differences between the two sintering techniques have been observed as shown in Figure 3. From this figure, we can find that the microwave sintering process in our experiment can be divided into three stages, and the microstructure evolution process was quite in accordance with coble's solid phase sintering theory. Just as it's stated in the theory, at the initial stage (as shown in Figure 3, from 0 to the 18th min), the grains gradually contacted with each other, the sintering necks formed, but the grains didn't grow up at this stage. At the middle stage (from the 18th to the 42nd min), the sintering necks grew further and the grain-boundary formed extensively, some grains began to grow, but the pores still linked together. At the final stage (from the 42nd to the 60th min), some of the pores were wrapped by grains, became isolated and spherical, and some of the pores were eliminated from the grains.

Though there were some phenomena coincident with the conventional sintering theory, there were some obvious microstructure evolution behaviors fairly different from the conventional sintering in our experiment, as shown in Figure 6. 1) From 0 to the 24th min, the shape of grains in the circle changed much faster than the other regions, and the sharp surface of these particles turned blunt, the grain marked with an arrow grew spherical. Moreover, the sintering neck growth was obviously observed in this region, yet this process was not found in the early stage of conventional sintering. 2) The larger particles marked with numbers from 1 to 6 grew much faster than the other small particles, yet this phenomenon has not been found in the conventional sintering experiments as well.

These phenomena could be explained by the theory of micro-focusing and polarization effects of microwave fields [15, 16], which considers that on a microscopic scale, the local electric fields can be disproportionately strong in certain regions close to grain boundaries and rough surfaces, leading to a highly non-uniform energy deposition and accelerated mass transfer rate. According to this theory, for the first phenomenon, SiC particles in the green circle were close to each other at the center of the region, and the electric fields were "collected" by these particles and focused into this small region as shown in Figure 6(d). So the local electric field intensity was tremendously stronger than the spatially averaged field, and the microstructure evolution process was accelerated as a result. For the second phenomenon, since the particles in this region were larger than the others, which means the electric fields ''collected'' by the larger ceramic particles were more than the smaller particles, so the electric fields that focused into the contact regions of larger particles would be stronger than those of the small particles, and consequently the microstructure evolution process of these larger particles was faster than the smaller ones.

4.2 Difference in the growth of sintering neck

Neck growth has great influence on shrinkage during microwave sintering and conventional sintering, and plays an important role in determining the main diffusion mechanism and calculating the diffusion coefficient of the material [17]. Therefore, many scholars have researched sintering neck growth under various mechanisms in conventional sintering theory, and various forms of neck growth equations have been obtained [18].

The dynamics of stable neck-growth summarized by Kucsynski is shown in the formula below:

$$\left(\frac{x}{a}\right)^n = \frac{F(T)}{a^m}t, \tag{1}$$

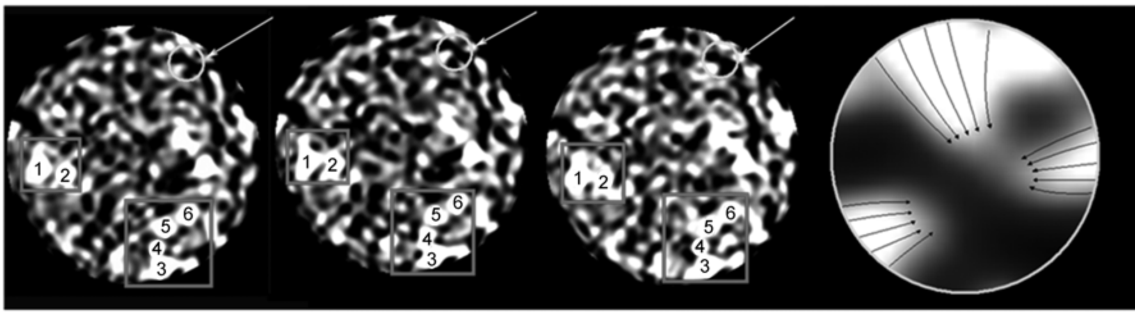

(a) $T=0$ min (b) $T=12$ min (c) $T=24$ min (d)

Figure 6 Microstructure evolution characteristic.

where x is the length of the sintering neck, a is the original radius of the grain, t is the time, m and n correspond to different diffusion mechanics, and $F(T)$ represents the function of temperature T. The formula indicates that exponential n represents the sintering neck growth exponent, the smaller the value of n, the faster the sintering neck growth rate. According to exponential criterion, such relationship is presented between different values of n and main mechanisms, such that n=2 indicates viscous flow, n=3 indicates evaporation-condensation, n=5 indicates bulk diffusion, n=6 indicates grain boundary diffusion, and n=7 indicates surface diffusion [19].

In this sintering theory, the curve of Ln(x)-Ln(t) will show a linear relationship. Some scholars have proved this conclusion by experiment in conventional sintering by the traditional non-online experimental techniques [20]. In our research group, we have also proved this theory by using the same material of SiC by the SR-CT technique in conventional sintering [19]. According to this theory, the relationship between Ln(x) and Ln(t) during microwave sintering process in our experiment was directly obtained as shown in Figure 7.

From Figure 7, it is found that there were three neck growth stages during the entire sintering process. From the beginning to 19.5 min, the sintering necks grew slowly. Then, the growth rate increased during the next stage from 19.5 to 49.5 min. By the end of the sintering process, the sintering neck growth rate slowed down. Besides, the curve between Ln(x) and Ln(t) shows a good linear relationship at each stage. This change could be observed directly from the cross-section images in Figure 3. However, the slope of the curve changed dramatically during the middle stage as shown in Figure 7 from the 3rd point to the 8th point. That means the sintering neck growth rate increased very much during this stage.

As we know, the theory of sintering neck growth is mainly used for the initial stage. However, during the middle stage, the microstructure evolution process becomes severe and the densification process mainly happens during this time, so it is difficult to observe the neck growth process online during this stage, and there are no reports about the related research work. Based on our experiment results, the sintering neck growth curve for the middle stage was obtained as shown in Figure 8. The linear fitting of the curve has been done as well. The exponent n acquired from the fitting line is 1/0.3142=3.1827, which approximates to 3. According to the exponential criterion, evaporation-condensation might be the main diffusion mechanism during this stage. As discussed in section 4.1, due to the existence of microwave fields, in certain regions such as inter-particle contact zones, pores, and rough grain surfaces, the local electric fields in these regions could be orders of magnitude stronger than the spatially averaged field. So materials in this region might gasify, and evaporation-condensation became the main diffusion mechanism. However, in the other study in our research group [19], we carried out the conventional sintering experiment on the same SiC material, with experiment condition all the same except for the heating manner. In that study, the exponent n obtained from the experiment was 7.87, which is larger than that obtained in the microwave sintering (n=3.1827). That means the two sintering techniques have different growth kinetics and main diffusion mechanisms. Because the two sintering techniques have different heating mechanisms, it is supposed that there must be some unclear mechanisms of sintering neck growth in microwave sintering that are different from the conventional sintering, and this is what we should study in the next research.

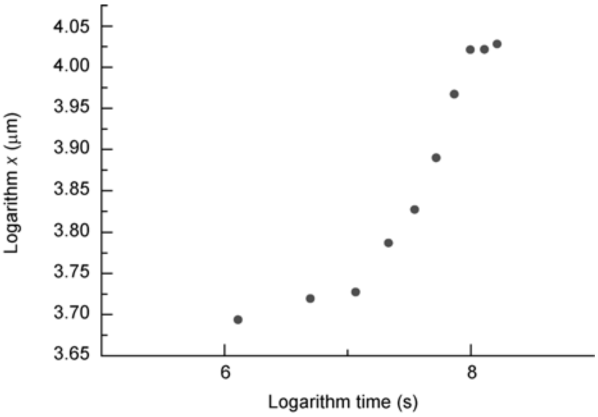

Figure 7 Double logarithmic curve of mean neck size and time.

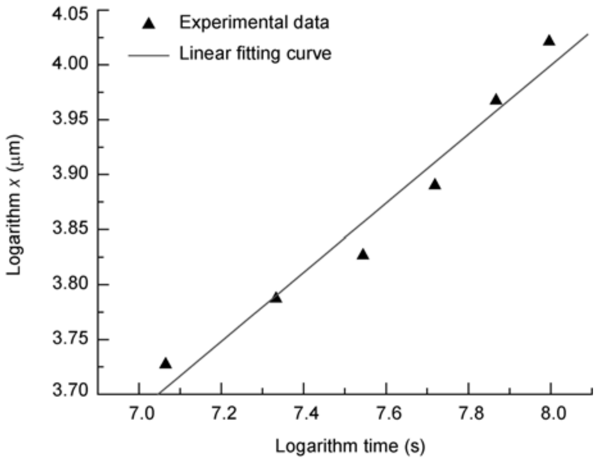

Figure 8 Linear fitting of Ln(x)-Ln(t) at middle stage.

5 Conclusions

The microstructure evolution of SiC was in-situ observed by the SR-CT technique during microwave sintering process.

1) A series of 2D and 3D reconstructed images of SiC powders during microwave sintering process were obtained. The microstructure evolution and many sintering phenomena of SiC powders during three sintering stages including

the shape change of grains and pores, the formation and growth of sintering necks, etc. were clearly observed.

2) Microstructure evolution processes of microwave sintering and conventional sintering were compared with each other, some obvious differences between them were observed from the reconstructed images, such as the bluntness of the sharp surface of grains near the contact regions, the larger particles grew faster than the smaller ones. The effects of micro-focusing of microwave fields were discussed to explain these phenomena.

3) Sintering neck sizes between SiC powders during microwave sintering process were calculated. The neck growth exponent was identified as n=1/0.3142, which is much larger than the value obtained from the conventional sintering experiment on the same material. However, the true reason for this phenomenon is not clear. Maybe, the effects of micro-focusing of electric fields played an important role. So further investigation on this aspect is needed.

This work was supported by the National Natural Science Foundation of China (Grant Nos. 10902108, 10732080, 10872190) and the National Basic Research Program of China ("973" Project) (Grant No. 2007CB936800). The authors warmly thank Xie Honglan for her help in preparing the experiments, as well as Niu Yu, Wang Luobin for fruitful discussions and assistance in conducting the experiments.

1 Xie Z, Yang J, Huang Y. Densification and grain growth of alumina by microwave processing. Mater Lett, 1998, 37: 215–220
2 Xie Z, Yang J, Huang X, et al. Microwave processing and properties of ceramics with different dielectric loss. J Eur Ceram Soc, 1999, 19: 381–387
3 Valecillos M C, Hirota M, Brite M E, et al. Microstructure and mechanical properties of microwave sintered silicon nitride. J Ceram Soc, 1998, 106: 1162–1166
4 Fujitsu S, Ikegami M, Hyashi T. Sintering of partically stabilized zirconia by microwave heating using ZnO-MnO_2-Al_2O_3 plates in a domestic microwaveoven. J Am Ceram Soc, 2000, 83: 2085–2087
5 Li X, Hu X F. Synchrotron radiation tomography for reconstruction of layer structures and interna damage of composite material. Chin J Laser B, 1999, B8(6): 503–550
6 Pyzalla A, Camin B, Buslaps T, et al. Simultaneous tomography and diffraction analysis of creep damage. Science, 2005, 308: 92–95
7 Chukalina M, Golosio B, Simionovici A, et al. X-ray tomography: how to evaluate the reconstruction quality. Spect Rochimica Acta Part B, 2004, 59: 1755–1758
8 Vagnon A, Lame O, Bouvard D, et al. Deformation of steel powder compacts during sintering: correlation between macroscopic measurement and in situ microtomography analysis. Acta Materialia, 2006, 54(2): 513–522
9 Lame O, Bellet D, Michiel M D, et al. Bulk observation of metal powder sintering by X-ray synchrotron microtomography. Acta Mater, 2004, 52: 977–984
10 Bernard D, Gendron D, Heintz J M, et al. First direct 3D visualization of microstructures evolution during sintering through X-ray computed microtomography. Acta Mater, 2005, 53: 121–128
11 Xu F, Hu X F, Niu Y, et al. In situ observation of grain evolution in ceramic sintering by SR-CT technique. Trans Nonfer Metal Soc Chin, 2009, 19(3): S684–S688
12 Seth G, Upadhyaya A. Microwave and conventional sintering of premixed and prealloyed Cu-12Sn bronze. Sci Sin, 2003, 35: 49–65
13 Brevala E, Chenga J P, Agrawal D K, et al. Comparison between microwave and conventional sintering of WC/Co composites. Mat Sci Eng A, 2005, 391: 285–295
14 Purushotham Y J, Ramesh P. Microwave sintering of Ni-Zn ferrites: comparison with conventional sintering. Mat Sci Eng B, 2003, 98: 269–278
15 Birnboim A, Calame J P, Carmel Y. Microfocusing and polarization effects in spherical neck ceramic microstructures during microwave processing. J Appl Phys, 1999, 85(1): 478–482
16 Calame J P, Birman A, Carmel Y, et al. A dielectric mixing law for porous ceramics based on fractal boundaries. J Appl Phys, 1996, 80(7): 3992–4000
17 Johnson D L. New method of obtaining volume, grain-boundary, and surface diffusion coefficient from sintering data. J Appl Phys, 1969, 40(1): 192–200
18 Kang S L. Sintering-Densification, "Grain Growth, and Microstructure" in Sintering Theory. London: Elsevier, 2005. 51–52
19 Niu Y, Xu F, Hu X F, et al. In situ investigation of the silicon carbide particles sintering. J Nanomater, doi: 10.115/2011/728617
20 Guo S J. "Powder Sintering Theory," In Sintering Theory. Beijing: Metallurgy Industry Press, 1998. 41–43